

THE STATUS OF NEUTRINO MASS

DAVID O. CALDWELL

*Institute for Nuclear and Particle
Astrophysics and Cosmology and
Physics Department, University of California,
Santa Barbara, CA 93106-9530, USA*

New experimental results, if correct, require at least one light sterile neutrino, in addition to the three active ones, to accommodate the mass differences required to explain the solar ν_e deficit, the anomalous ν/e ratio produced by atmospheric neutrinos, and either the candidate events for $\nu_\mu \rightarrow \nu_e$ (or $\bar{\nu}_\mu \rightarrow \bar{\nu}_e$) from the LSND experiment, or the possible need for a hot component of dark matter. This neutrino mass pattern can not only accommodate all these four requirements, but also provide a robust solution to a problem presently making heavy-element synthesis by supernovae impossible and resolve a possible discrepancy between big bang nucleosynthesis theory and observations.

1 Introduction

The evidence is now becoming very strong for a particular pattern of neutrino masses, one which requires at least one light sterile neutrino. Either some of the experimental results are wrong, or we are forced to this conclusion. This experimental evidence will be reviewed briefly, with emphasis on very new results, and the consequences for neutrino mass examined. Indirect evidence for the same mass pattern from dark matter, supernova nucleosynthesis, and big-bang nucleosynthesis will then be presented, showing the widespread effect of massive neutrinos. This mass pattern should, however, produce some apparently negative results from current experiments which could have a deleterious effect on the field unless they are properly anticipated.

2 Indications for Nonzero Neutrino Mass

2.1 Solar Neutrino Deficit

All solar neutrino experiments observe fewer electron neutrinos (ν_e) than solar models predict. In addition, because the three types of experiments cover different ν_e energy ranges and hence sample differently the contributions from the various nuclear processes producing neutrinos, there is an energy-dependent discrepancy well illustrated in Fig. 1(a). This figure, from a very complete review,¹ shows the relationship between neutrino fluxes from ⁷Be and ⁸B neutrinos as measured in the three types of experiments. The SAGE² and GALLEX³ radiochemical experiments go to the lowest energy and hence measure all of

both fluxes (designated “Ga”), while the Homestake⁴ radiochemical experiment measures all of the ⁸B spectrum but only part of the ⁷Be flux (labeled as “Cl”), and the Kamiokande⁵ and Super-Kamiokande⁶ scattering experiments measure only ⁸B flux (designated as “Kam”). Results from all three actually intersect at a negative value of the ⁷Be flux, yet ⁸B is produced from $^{7}\text{Be} + \text{p} \rightarrow ^{8}\text{B} + \gamma$. This problem cannot be avoided by one of the experiments being wrong. The discrepancy between a standard solar model⁷ and all three types of experiments is shown by the point with error bars in the upper right-hand corner indicating predicted fluxes. Solar models which drastically change solar properties do not solve the problem. Recent very accurate helioseismology measurements severely constrain solar models and apparently rule out any astrophysical explanation⁸ of the solar neutrino discrepancies.

A good solution to the solar ν_e deficit is provided by oscillation into ν_μ , ν_τ , or ν_s , a sterile neutrino, one not having the normal weak interactions. While this can be a vacuum oscillation, requiring a mass-squared difference $\Delta m^2 \sim 10^{-10} \text{ eV}^2$ and large mixing between ν_e and the other neutrino, more favored is a matter-enhanced MSW⁹ type of oscillation. For a ν_μ or ν_τ final state, $\Delta m_{ei}^2 \sim 10^{-5} \text{ eV}^2$ and mixings either $\sin^2 2\theta_{ei} \sim 6 \times 10^{-3}$ or ~ 0.6 are possible, while only the former is allowed for ν_s . The main change as a result of the new Super-Kamiokande data is that the lack of a day-night effect has reduced the parameter space for the large-angle solution for the ν_μ or ν_τ final state.¹⁰ The Super-Kamiokande result which will become of prime importance as the error bars are reduced is shown in Fig. 1(b). This energy spectrum could not only choose among the oscillation solutions—and it is well fit at this stage by the MSW small-angle solution—but also it may be the one means of proving that oscillations are occurring, as will be explained later.

2.2 Atmospheric Neutrino Deficit

Pions produced in the atmosphere would decay via $\pi \rightarrow \mu + \nu_\mu$, $\mu \rightarrow e + \nu_\mu + \nu_e$, so that one would expect $N(\nu_\mu + \bar{\nu}_\mu) = 2N(\nu_e + \bar{\nu}_e)$, with a small correction for K decays. The $(\nu_\mu + \bar{\nu}_\mu)/(\nu_e + \bar{\nu}_e)$ ratio would be observed in underground experiments as μ^\pm/e^\pm , and the result is far from the expected value. Because the calculated μ^\pm and e^\pm individual fluxes are known to $\sim 15\%$, whereas much of the uncertainty drops out in the ratio, the experiments utilize $R = (\mu/e)_{\text{Data}}/(\mu/e)_{\text{Calc}}$. Values of R for many experiments are shown in Fig. 2(a). While it once appeared that there was a discrepancy between water Cherenkov detectors and tracking calorimeters,¹¹ the Soudan II results¹² agree with those from IMB¹³, Kamiokande¹⁴, and Super-Kamiokande¹⁵. In addition, the MACRO detector finds a similar deficiency of muons, although

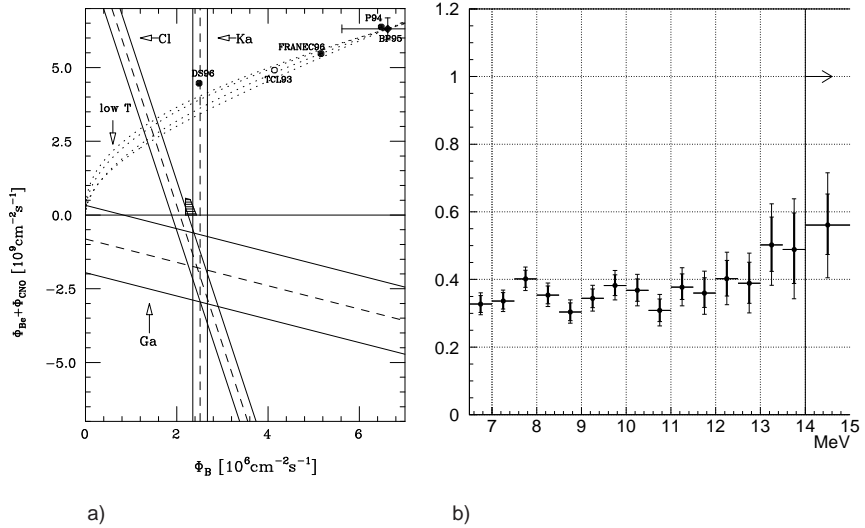


Figure 1: a). The ^8B and ^7Be (+ CNO) neutrino fluxes for standard neutrinos. The dashed (solid) lines correspond to central ($\pm 1\sigma$) experimental values for the chlorine (Cl), gallium (Ga) and Kamiokande (Ka) experiments. The hatched area corresponds to a region within 2σ from each experimental result. The predictions of solar models are shown, with the one⁷ with error bars being most often referenced. The dotted lines indicate the behavior of non-standard solar models with low central temperature. b).The Super-Kamiokande solar neutrino energy spectrum with dark error bars for statistics and light error bars including systematics, mainly determined by the energy calibration.

their angular distribution is ambiguous, slightly favoring a neutrino oscillation explanation of the lack of muons.¹⁶

While the statistical evidence for R being less than unity is now quite compelling, it is the angular distributions of the μ and e events which provide the primary evidence that this deviation of R from unity is explained by neutrino oscillations. This non-flat distribution with angle of R was first observed in the high-energy (> 1.3 GeV) event sample from Kamiokande, but has now been confirmed with better statistics in the similar data sample from Super-Kamiokande, as shown in Fig. 2(b). The data fits an oscillation hypothesis, using $\Delta m^2 = 5 \times 10^{-3} \text{ eV}^2$, $\sin^2 2\theta = 1$ (as a sample, but not a best, fit) and is far from a non-oscillation, flat distribution. The low-energy (< 1.3 GeV) sample also agrees with the same oscillation parameters, but this should be a

much shallower angle dependence, and hence it is statistically less compelling, as is also shown in the figure.

The disappearance of the muon neutrinos could be due to $\nu_\mu \rightarrow \nu_\tau$ or $\nu_\mu \rightarrow \nu_e$, with $\nu_\mu \rightarrow \nu_s$ being unlikely because the large mixing angle would bring the ν_s into equilibrium in the early universe, possibly providing too many neutrinos to get agreement between predictions of nucleosynthesis and observed light element abundances. The Super-Kamiokande observations of e and μ compared to calculated fluxes, as well as the individual e and μ angular distributions, as shown in Fig. 3(a), makes $\nu_\mu \rightarrow \nu_e$ very unlikely. Note the e distributions are like the non-oscillation Monte Carlo, whereas those for μ agree with the oscillation prediction. The recent results of the CHOOZ nuclear reactor experiment,¹⁷ shown in Fig. 3(b), which does not see evidence of ν_e disappearing in the appropriate region of Δm^2 and $\sin^2 2\theta$, confirms that the atmospheric effect is very unlikely to be $\nu_\mu \rightarrow \nu_e$. On the basis that the Super-Kamiokande observed values of R and angular distributions of R are due to $\nu_\mu \rightarrow \nu_\tau$, the likely value of Δm^2 is definitely much larger than that required for an explanation of the solar neutrino deficit, and the flavors of neutrinos cannot be the same in the two cases. Turning now to the third possible manifestation of neutrino mass, we shall see that the atmospheric Δm^2 is much smaller than that required for the LSND experiment, and hence that three distinctly different values of neutrino mass differences are required.

2.3 Evidence for Neutrino Oscillations from the LSND Experiment

The LSND accelerator experiment uses a decay-in-flight ν_μ beam of up to ~ 180 MeV from $\pi^+ \rightarrow \mu^+ \nu_\mu$ and a decay-at-rest $\bar{\nu}_\mu$ beam of less than 53 MeV from the subsequent $\mu^+ \rightarrow e^+ \nu_e \bar{\nu}_\mu$. The 1993+1994+1995 data sets included 22 events of the type $\bar{\nu}_e p \rightarrow e^+ n$, based on identifying an electron between 36 and 60 MeV using Cherenkov and scintillation light and tightly correlated with a γ ($< 0.6\%$ accidental rate) from $np \rightarrow d\gamma$ (2.2 MeV), whereas only 4.6 ± 0.6 such events were expected from backgrounds.¹⁸ The chance that these data, using a water target, result from a fluctuation is $< 10^{-7}$. Subsequent data sets from 1996+1997 taken with an iron target gave a similar oscillation probability with much worse statistical accuracy. More importantly, the first data sets (1993–5) yielded events from π decay in flight consistent with being from $\nu_\mu \rightarrow \nu_e$. These were similar in number to those from $\bar{\nu}_\mu \rightarrow \bar{\nu}_e$, but with about twice the background, since the observed process ($\nu_e C \rightarrow e^- X$) gave only one signal instead of two. While the fluctuation probability in this case is only $\sim 10^{-2}$, the two ways of detecting oscillations are essentially independent.¹⁹

While the $\nu_\mu \rightarrow \nu_e$ results are consistent with those from $\bar{\nu}_\mu \rightarrow \bar{\nu}_e$,

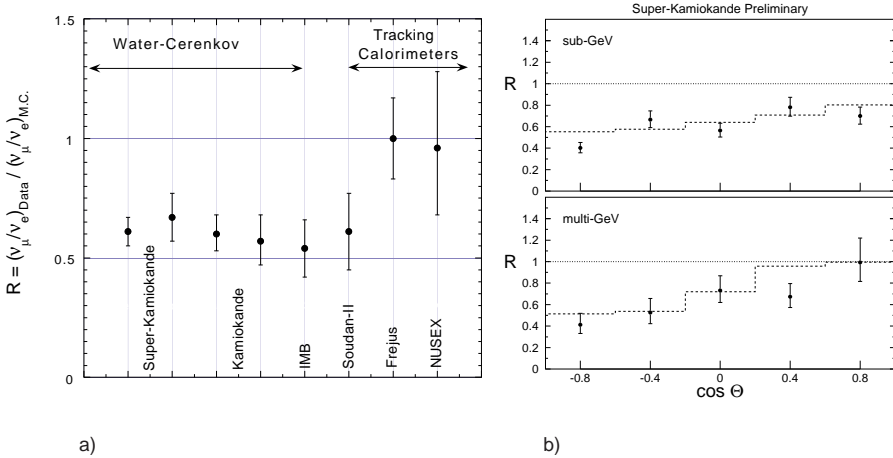


Figure 2: a) The double ratio of ν_μ/ν_e from data to that from calculations for atmospheric neutrinos for various detectors. Note that Super-Kamiokande and Kamiokande each have two independent data sets, above and below 1.3 GeV; b) The ratio $(\mu/e)_{\text{DATA}}/(\mu/e)_{\text{MC}}$ for sub-GeV and multi-GeV atmospheric neutrino samples from Super-Kamiokande, as a function of zenith angle. Neutrinos coming from below are at $\cos \Theta = -1$. The dashed line shows the expected shape for $\nu_\mu \rightarrow \nu_\tau$ oscillation with $\sin^2 2\theta = 1$ and $\Delta m^2 = .005 \text{ eV}^2$.

only the latter have sufficient statistics to provide restrictions on the value of Δm^2 . These $\bar{\nu}_\mu$ results interpreted as a two-generation oscillation have been presented¹⁸ in a plot like Fig. 4(a), except that comparisons were made to limits from other experiments. Figure 4(a) is the correct way to determine favored regions of Δm^2 as a function of the mixing angle, θ . The plot utilizes all the information about the events, in particular the neutrino energy, E , and the distance of the event from the source, L . In order to increase the range of L/E , values of E down to 20 MeV were used. Figure 4(a) shows contours at 2.3 and 4.5 log-likelihood units from the maximum. If this were a gaussian distribution, which it is not (its integral being infinite), the contours would correspond to 90% and 99% likelihood levels, but in addition they have been smeared to account for some systematic errors. Comparison to the KARMEN experiment,²⁰ which presents results in a similar way, shows no conflict, but if limits are plotted (as they are in Ref. 18) on this graph from E776 at BNL²¹ and the Bugey reactor experiment,²² then one might conclude that the only allowed Δm^2 region is 0.2–3 eV². If instead an 80% confidence level band is calculated to compare with the 90% confidence level limits of those experiments using, as they do, just numbers of events (i.e., not using the L/E information)

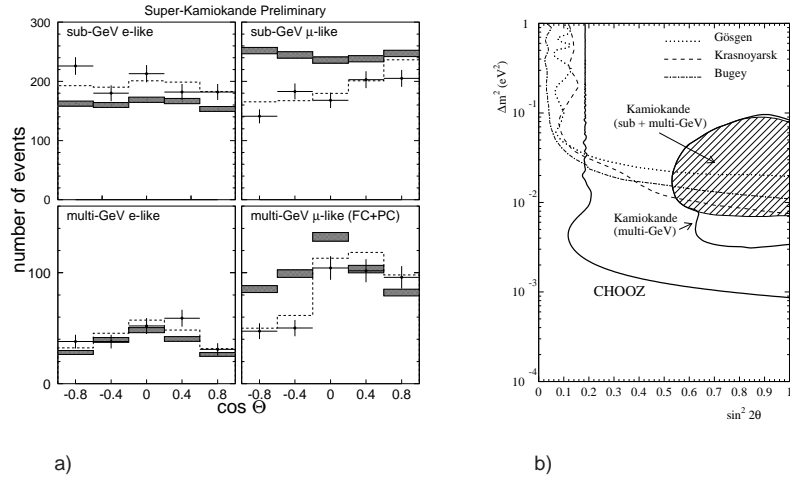


Figure 3: a) The rate of μ -like and e -like events in the sub-GeV and multi-GeV atmospheric neutrino samples from Super-Kamiokande, as a function of zenith angle. The solid histograms are the Monte Carlo expectation with no neutrino oscillation; the thickness represents the statistical uncertainty in the Monte Carlo sample. The dashed line shows the expected shape for $\nu_\mu \rightarrow \nu_\tau$ oscillation with $\sin^2 2\theta = 1$ and $\Delta m^2 = .005$ eV². b) The 90% C.L. exclusion plot for CHOOZ, compared with previous experimental limits and with the Kamiokande allowed region for ν_e disappearance.

and using only the 36–60 MeV region with its much lower background, then there is no conflict with other experiments above 0.2 eV², up to the recent limit of about 10 eV² from the NOMAD experiment,²³ as shown in Fig. 4(b).

3 Pattern of Neutrino Masses Required by Experiments

Because measurements of the width of the Z^0 boson require that there be only three light neutrinos coupled to the Z^0 , it would be desirable to explain the phenomena described in the previous section in terms of oscillations among those three neutrinos. Since the flavors are constrained, one has to invoke indirect neutrino oscillations, so LSND could be observing $\nu_\mu \rightarrow \nu_\tau \rightarrow \nu_e$, for example, with the largest (dominant) Δm^2 being between ν_μ and ν_τ or ν_e and ν_τ , with a small $\Delta m_{e\mu}^2$. There is still the problem that three neutrinos provide only two mass-squared differences, so one might assume $\Delta m_{\text{solar}}^2 \approx \Delta m_{\text{atmos.}}^2$, as did Acker and Pakvasa,²⁴ requiring both processes to be dominantly $\nu_e \rightleftharpoons \nu_\mu$. This leads to requiring the solar ν_e deficit to be energy independent, in conflict

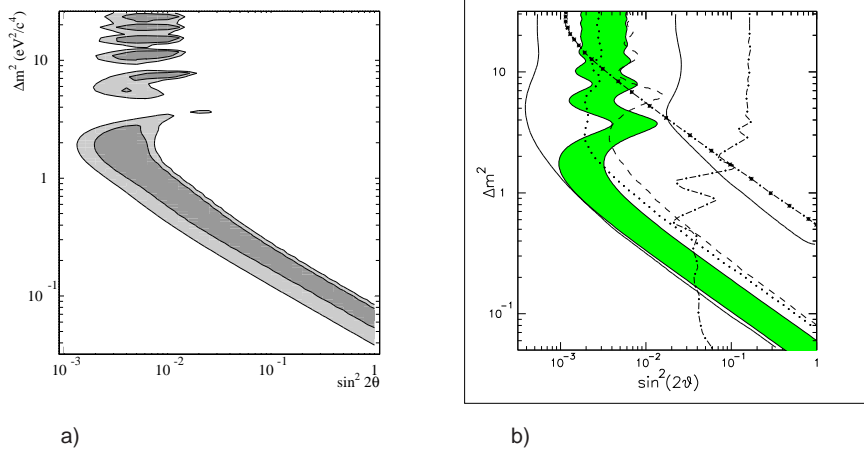


Figure 4: a) Mass-squared difference (Δm^2) vs. degree of mixing ($\sin^2 2\theta$) assuming a two-neutrino oscillation explanation of the LSND beam-excess data. Shown are regions of Δm^2 favored using the energy (from 20 to 60 MeV) and distance from the source of each event.b) As in (a) but the LSND $\bar{\nu}_\mu$ data here provide an 80% C.L. band, which is to be compared with the LSND ν_μ result (solid lines), KARMEN (dashes), E776 (dots), Bugey (dash-dot), and NOMAD.

with the data (see, e.g., Fig 1). This is a problem besetting most three-neutrino schemes. The Acker-Pakvasa model is essentially ruled out by the CHOOZ result of Fig. 3(b), as well as the angular distributions of Fig. 3(a).

The only other alternative for three neutrinos is making $\Delta m_{\text{atmos.}}^2 = \Delta m_{\text{LSND}}^2$. This was suggested by Cardall and Fuller,²⁵ who used the indirect oscillation for LSND and made $\Delta m_{e\tau}^2 \approx \Delta m_{\mu\tau}^2 \approx 0.3$ eV², since the solar $\Delta m_{e\mu}^2 \approx 10^{-5}$ eV² is so small. This scheme has no difficulty with the solar data, but could be in some conflict with limits from neutrinoless double beta decay, if one wants to provide a hot dark matter component, since $m_{\nu_e} \approx m_{\nu_\mu} \approx m_{\nu_\tau} \approx 1.6$ eV, as will be explained in the next section. This scheme, the three-neutrino pattern having the least conflict with data,²⁶ is definitely ruled out by the Super-Kamiokande data shown in Figs. 2(b) and 3(a).

There is no way the Δm^2 required by LSND can be the same as that needed for the atmospheric anomaly.

Either the experiments are wrong or one is forced to invoke another light neutrino, a sterile one which does not have the normal weak interactions and hence does not couple to the Z^0 . Then the solar ν_e deficit is a result of $\nu_e \rightarrow \nu_s$, with $\Delta m_{es}^2 \lesssim 10^{-5}$ eV 2 , the atmospheric ν_μ/ν_e ratio is explained by $\nu_\mu \rightarrow \nu_\tau$, with $\Delta m_{\mu\tau}^2 \sim 10^{-2} - 10^{-3}$ eV 2 , and the LSND observation is caused by $\nu_\mu \rightarrow \nu_e$, with 0.2 eV $^2 \lesssim \Delta m_{e\mu}^2 \lesssim 10$ eV 2 . The information considered so far requires this and only this, but we shall see that a wide range of phenomena can be explained for a more specified value of $\Delta m_{e\mu}^2$ and for which the sterile neutrino is a necessity.

4 Implications of the Four-Neutrino Mass Pattern

4.1 Dark Matter

This four-neutrino mass pattern was first proposed²⁷ five years ago, well before there were any results from LSND. The motivation then was to explain the solar and atmospheric deficits and the apparent need for some of the missing mass of the universe to be in the form of neutrinos. The neutrino mass required is $94 h^2 \Omega F_\nu$, where h is the Hubble constant in units of $100 \text{ km}\cdot\text{s}^{-1}\cdot\text{Mpc}^{-1}$, Ω is the density of the universe in units of the critical density, and F_ν is the neutrino fraction of Ω . For example, if $h = 0.5$, $\Omega = 1$, and $F_\nu = 0.2$, then 4.7 eV of neutrino mass is needed. Before LSND it was suggested²⁷ that there were only two ways to get the needed neutrino mass as well as explain the solar and atmospheric deficits: 1) the four-neutrino scheme with ν_e and ν_s light ($\ll 1$ eV), and ν_μ and ν_τ sharing the dark matter role ($\sim 2-3$ eV each), or 2) $\nu_e \rightarrow \nu_\mu$ for solar, $\nu_\mu \rightarrow \nu_\tau$ for atmospheric, and all three neutrinos providing dark matter (~ 1.6 eV each). After LSND the latter scheme failed the flavor constraint, so indirect oscillations had to be invoked, and it became the Cardall-Fuller proposal²⁵. Now only the former (four-neutrino) scheme remains. The main point of mentioning this history is to emphasize that the four-neutrino pattern can be motivated even without LSND.

The dark matter part of that motivation arises because relic neutrinos remain ($\sim 100/\text{cm}^3$ per neutrino flavor) from the early universe, and if they have even a few eV in mass they could solve the main problem of cold dark matter (CDM) models, namely production of much more structure on small scales than is observed. This results from baryons being readily accreted to overdense regions of the slowly moving CDM. CDM models give a quite good approximation to the structure of the universe over a wide range of distance scales, but when an absolute normalization of the predictions was provided by

the COBE data, the overproduction of small-scale structure became apparent. Since the free streaming of neutrinos could reduce density fluctuations on small scales, the addition of 30% neutrinos (i.e., $F_\nu = 0.3$) allowed fitting structure on all scales very well. The problem with this early cold+hot dark matter model²⁸ was that this damping of density perturbations also caused structure to form too late. Reducing the neutrino content to $\sim 20\%$ allowed early enough structure formation.²⁹ With all the mass (4.7 eV) in one neutrino species, this otherwise successful model ($C\nu$ DM) overproduced clusters of galaxies. In other words, the $C\nu$ DM model worked well at all distance scales except $\sim 10h^{-1}$ Mpc. With the motivation of the four-neutrino model discussed above, simulations were tried in which the dark matter was shared between two 2.4 eV neutrinos, yielding a quite unexpected result.³⁰ While 4.7 eV in one neutrino species or two makes essentially no difference at very large or very small scales, at $\sim 10h^{-1}$ Mpc the larger free-streaming length of the 2.4 eV neutrinos washes out density fluctuations and hence lowers the abundance of galactic clusters.

This $C\nu^2$ DM model with two, 2.4 eV neutrinos fits structure information on all scales. In every aspect of simulations done subsequently the two-neutrino dark matter gives the best results. For example, a single neutrino species (as well as low- Ω models) overproduce void regions between galaxies, whereas the $C\nu^2$ DM model agrees with observations.³¹ Note that the $C\nu^2$ DM model is compatible with all the information mentioned in Section 2 provided $\Delta m_{e\mu}^2$ from LSND is $\sim 6\text{--}8$ eV². This happens to be the region of Fig. 4(a) corresponding to the second oscillation maximum for $\bar{\nu}_\mu \rightarrow \bar{\nu}_e$ and the first oscillation maximum (Fig. 4(b)) for $\nu_\mu \rightarrow \nu_e$, so if this is the correct Δm^2 the target-to-detector distance for LSND is extremely fortuitous.

The $C\nu^2$ DM model works if $\Omega = 1$ and $h \lesssim 0.6$. Not long ago large values of h were popular, providing a universe age crisis. Formerly high values of h have been reduced, and the Hipparcos satellite measurements³² of stellar parallaxes reduced both the age of the universe and h values. Now there is no conflict between the age of the oldest stars and the currently favored $h \sim 0.6$, with many measurements of h coming out even lower than that.

The latest bandwagon is a low- Ω universe, contrary to the expectation of almost all models of a period of inflationary expansion of the universe which require $\Omega = 1$ and explain the isotropy of the cosmic microwave background, the flatness problem, lack of monopoles, and the origin of large-scale structure. To have a density not now near zero or infinity requires $\Omega + \Lambda = 1$, where Λ is an arbitrary cosmological constant having little or no theoretical justification. One reason low- Ω is popular is based on assuming that galactic clusters are representative of the universe as a whole, using X-ray measurements of the gas in clusters to determine the fraction of mass in baryons, F_B , and taking the

value of the baryon density in the universe, Ω_B , as determined by primordial He abundance to get $\Omega = \Omega_B/F_B = 0.05/0.15 = 0.3$. The X-ray measurements, depending on a collision process, could give an overestimate if the gas is clumped, so that recent measurements of the Sunyaev-Zeldovitch effect³³ are more reliable and give $F_B = (0.06 \pm 0.01)h^{-1}$. A particularly sensitive determination of the baryon-to-photon ratio at the time of nucleosynthesis is provided by the primordial deuterium to hydrogen ratio, D/H. There were conflicting values of D/H in very high red-shift clouds, but these are now resolved in favor of low D/H,³⁴ from which one gets $\Omega_B = (0.024^{+0.006}_{-0.005})h^{-2}$. Then $\Omega = 0.4h^{-1}$, so $\Omega = 0.7\text{--}0.8$, quite consistent with $\Omega = 1$, since a large-scale simulation³⁵ of measured galactic cluster properties yields values like $\Omega = 0.5$ when the input to the simulation is $\Omega = 1$. This discrepancy could explain some other observations apparently favoring low Ω .

Particularly important to note is that if the LSND measurement is confirmed by another experiment which finds $\Delta m_{e\mu}^2 \sim 6\text{--}8 \text{ eV}^2$, the existence of one 2–3 eV neutrino would require large Ω .³⁰ Such a neutrino washing out density fluctuations in the early universe would not allow sufficient structure to form for low Ω , making $\Omega = 1$ highly probable. Thus a neutrino experiment could settle the much-disputed issue of the ultimate fate of the universe.

4.2 Heavy-Element Nucleosynthesis in Supernovae

While the $\Delta m_{e\mu}^2 \sim 6\text{--}8 \text{ eV}^2$ value is necessary for the successful two-neutrino dark matter, it causes an apparent conflict with the production of heavy elements in supernovae. This *r*-process of rapid neutron capture occurs in the outer neutrino-heated ejecta of Type II supernovae. The existence of this process would seem to place a limit on the mixing of ν_μ and ν_e because energetic ν_μ ($\langle E \rangle \approx 25 \text{ MeV}$) coming from deep in the supernova core could convert via an MSW transition to ν_e inside the region of the *r*-process, producing ν_e of much higher energy than the thermal ν_e ($\langle E \rangle \approx 11 \text{ MeV}$). The latter, because of their charge-current interactions, emerge from farther out in the supernova where it is cooler. Since the cross section for $\nu_e n \rightarrow e^- p$ rises as the square of the energy, these converted energetic ν_e would deplete neutrons, stopping the *r*-process. Calculations³⁶ of this effect limit $\sin^2 2\theta$ for $\nu_\mu \rightarrow \nu_e$ to $\lesssim 10^{-4}$ for $\Delta m_{e\mu}^2 \gtrsim 2 \text{ eV}^2$, in conflict with compatibility between the LSND result and a neutrino component of dark matter.

The sterile neutrino, however, can not only solve this problem, but also rescue the *r*-process itself. While recent simulations have found the *r*-process region to be insufficiently neutron rich, very recent realization of the full effect of α -particle formation has created a disaster for the *r*-process.³⁷ The initial

difficulty of too low entropy (i.e., too few neutrons per seed nucleus, like iron) has now been drastically exacerbated by calculations³⁷ of the sequence in which all available protons swallow up neutrons to form α particles, following which $\nu_e n \rightarrow e^- p$ reactions create more protons, creating more α particles, and so on. The depletion of neutrons by making α particles and by $\nu_e n \rightarrow e^- p$ rapidly shuts off the *r*-process, and essentially no nuclei above $A = 95$ are produced.

The sterile neutrino would produce two effects.³⁸ First, there is a zone, outside the neutrinosphere (where neutrinos can readily escape) but inside the $\nu_\mu \rightarrow \nu_e$ MSW (“LSND”) region, where the ν_μ interaction potential goes to zero, so a $\nu_\mu \rightarrow \nu_s$ transition can occur nearby, depleting the dangerous high-energy ν_μ population. Second, because of this ν_μ reduction, the dominant process in the MSW region reverses, becoming $\nu_e \rightarrow \nu_\mu$, dropping the ν_e flux going into the *r*-process region, hence reducing $\nu_e n \rightarrow e^- p$ reactions and allowing the region to be sufficiently neutron rich. This rescuing scenario—the only robust one which has been found after many attempts—works even better if the MSW region is inside the radius at which the weak interactions freeze out. This density requirement is well satisfied for $\Delta m_{e\mu}^2 \sim 6$ eV², a value which cannot be reduced appreciably.

4.3 Light-Element Nucleosynthesis in the Early Universe

Another possible indication for the existence of the sterile neutrino comes from the big-bang production of light elements. The apparent incompatibility of determinations of the baryon-to-photon ratio (hence fraction of baryons or the number of light degrees of freedom, like neutrinos) on the basis of ${}^4\text{He}$ abundance as opposed to the low D/H ratio, indirectly alluded to in Sec. 4.1, could also be resolved by the sterile neutrino. While not the most precise way of doing so, this issue is more easily discussed in terms of the effective number of light neutrinos, N_{eff} , in equilibrium at the time of nucleosynthesis. To reconcile the deduced primordial ${}^4\text{He}$ abundance with the low D/H values a universe expansion rate at the time of decoupling of the neutron-to-proton ratio would have to be governed by $N_{\text{eff}} = 1.9 \pm 0.3$, or put another way, standard big-bang nucleosynthesis is said to be excluded at the 99.9% C.L.³⁹ Adding sterile neutrinos would seem only to make the problem worse. Foot and Volkas have suggested,⁴⁰ however, that the lepton number asymmetry created by transitions of $\bar{\nu} \rightarrow \bar{\nu}_s$ could lead to a significant excess of ν_e over $\bar{\nu}_e$, so that the n/p ratio would be depleted prior to the decoupling of the $\nu_e n \rightarrow e^- p$ reaction, leading to the production of less ${}^4\text{He}$. This would produce the same result as artificially changing the universe expansion rate by making $N_{\text{eff}} < 3$. This lepton asymmetry comes about because the conditions for a given MSW

transition will not produce both $\nu \rightarrow \nu_s$ and $\bar{\nu} \rightarrow \bar{\nu}_s$, and the scarceness of initial sterile neutrinos makes the dominant MSW transition active \rightarrow sterile and not the other way around.

The small Δm^2 of the solar case makes $\bar{\nu}_e \rightarrow \bar{\nu}_s$ have a negligible effect. However, $\bar{\nu}_\mu \rightarrow \bar{\nu}_s$ and/or $\bar{\nu}_\tau \rightarrow \bar{\nu}_s$ with $\Delta m^2 \sim 6\text{--}8\text{ eV}^2$ could create a large lepton asymmetry which can be transformed to ν_e through $\nu_\mu \rightarrow \nu_e$ and/or $\nu_\tau \rightarrow \nu_e$. Foot and Volkas find⁴⁰ that $\Delta m^2 > 3\text{ eV}^2$ is required since at a lesser Δm^2 the MSW density would be achieved at too late a time. This restriction is very like that of the supernova nucleosynthesis case, again hinting that the LSND result lies in the upper range of the allowed region. There is also the interesting possibility that nearly mass-degenerate ν_μ and ν_τ could produce about double the effect Foot and Volkas find, $\delta N_{\text{eff}} = -0.5$, and hence 3 active neutrinos could give $N_{\text{eff}} \approx 2$ for the 4-neutrino scheme described above.

5 Conclusions

Either one of the three experimental evidences for neutrino oscillations (solar ν_e deficit, anomalous atmospheric ν_μ/ν_e ratio, and LSND events, or as an alternative to the last, the need for a neutrino component of dark matter) is wrong or a neutrino mass pattern is required which includes at least one light sterile neutrino. This pattern utilizes $\nu_e \rightarrow \nu_s$ for the solar effect with $\Delta m_{es}^2 \lesssim 10^{-5}\text{ eV}^2$, $\nu_\mu \rightarrow \nu_\tau$ for the atmospheric case with $\Delta m_{\mu\tau}^2 \sim 10^{-2}\text{--}10^{-3}\text{ eV}^2$, and $\nu_\mu \rightarrow \nu_e$ for LSND's events with $0.2 < \Delta m_{e\mu}^2 < 10\text{ eV}^2$. If in addition the ν_e and ν_s are $\ll 1\text{ eV}$ and the ν_μ and ν_τ are $\sim 2.4\text{ eV}$ each (so that $\Delta m_{e\mu}^2 \sim 6\text{--}8\text{ eV}^2$) then this pattern also provides the best hot+cold dark matter model, and it fits universe structure on all scales. The ν_s provides the only known robust solution to an otherwise disastrous failure of the r -process of heavy element nucleosynthesis in supernovae. It could also aid the p -process nucleosynthesis and supernova blow-up at an earlier stage in the supernova process. Finally the ν_s could bring about concordance in the present discrepancy between the primordial abundance of ${}^4\text{He}$ and the D/H ratio, probably especially with nearly mass degenerate ν_μ and ν_τ . Both the beneficial effects for the r -process and for big-bang nucleosynthesis require a large $\Delta m_{e\mu}^2$, compatible with that needed for dark matter.

Despite the appeal of being able to explain so many things with this mass pattern, there is reluctance among some to accept light sterile neutrinos. Theoretically, sterile neutrinos are quite usual. Indeed, the most natural is to have one for each generation, but generally these are very heavy, and the main problem is to make at least one of them light. Several schemes have been suggested, and a particularly appealing one is that by Langacker⁴¹ which occurs in a class

of string models.

Finally, a warning: this otherwise desirable neutrino mass pattern should lead to negative experimental results which could have a stultifying effect on this field. The KARMEN experiment²⁰ is touted as being able to check the LSND result, and it can do so except in the crucial ~ 6 eV² region. Since its source-to-detector distance is half that of LSND, this Δm^2 is at an oscillation minimum, as is clear in Fig. 4(b). The null result from KARMEN would soon be followed by an even more devastating negative result from SNO. The SNO comparison of charge-current events to neutral-current events would be consistent with no neutrino oscillation, which is also what should be expected from a solar $\nu_e \rightarrow \nu_s$ transition. The CHORUS and NOMAD experiments, designed for single-neutrino dark matter, are sensitive in the wrong Δm^2 region for $\nu_\mu \rightarrow \nu_\tau$ and will get a null result, although a search for $\nu_e \rightarrow \nu_\tau$ could be interesting. If presently planned long-baseline oscillation experiments proceed, it is possible that they will also fail to show positive results, since the atmospheric results from Super-Kamiokande may indicate a Δm^2 an order of magnitude smaller than that for which the experiments were originally designed. The subject of neutrino mass has had a bad history, and these negative results could lead to total disbelief in earlier positive results and likely withdrawal of support for future work.

The situation can be helped by anticipation of these null results—and that is the main point of this paper—and by doing the difficult experiments which could get the field out of trouble. First, the energy spectrum of solar neutrinos, as in Fig. 1(b), and the angular distribution of atmospheric ν_μ/ν_e must be measured as well as possible to provide convincing evidence of oscillations. Second, the $\Delta m_{e\mu}^2 \sim 6\text{--}8$ eV² region of LSND must be checked. It would be highly desirable to change the source-to-detector distance in that experiment, but an independent measurement would be even better. We are on the verge of a significant leap forward in understanding a wide range of phenomena, making it essential to avoid this possible blocking of progress.

Acknowledgments

Appreciation is due D. Bauer, G. Fiorentini, N. Hata, E. Kearns, C. Lane, G. McLaughlin, B. Ricci, R. Svoboda, and S. Yellin for supplying figures. It is a pleasure to thank G.M. Fuller, R.N. Mohapatra, J.R. Primack, and Y.-Z. Qian for extensive contributions to different parts of this paper. The U.S. Department of Energy is thanked for partial support of this work. Special thanks goes to L. Roszkowski for the invitation to give this talk at his excellent COSMO-97 conference.

References

1. V. Castellani *et al.*, *Phys. Rep.* **281**, 309 (1997).
2. J.N. Abdurashitov *et al.*, *Phys. Lett. B* **328**, 234 (1994); *Nucl. Phys. B* **38**, 60 (1995); *Phys. Rev. Lett.* **77**, 4708 (1996).
3. P. Anselmann *et al.*, *Phys. Lett. B* **327**, 377 (1994); *Phys. Lett. B* **342**, 440 (1995); *Phys. Lett. B* **357**, 237 (1995); W. Hampel *et al.*, *Phys. Lett. B* **388**, 384 (1996).
4. B.T. Cleveland *et al.*, *Nucl. Phys. B* (Proc. Suppl.) **38**, 47 (1995).
5. Y. Fukuda *et al.*, *Phys. Rev. Lett.* **77**, 1683 (1996).
6. Y. Totsuka, *Proc. Lepton-Photon Symposium*, Hamburg 1997 (in press).
7. J.N. Bahcall and M.H. Pinsonneault, *Rev. Mod. Phys.* **67**, 781 (1995).
8. W.C. Haxton's conclusion at *Conference on Solar Neutrinos*, Inst. for Theor. Phys., Univ. of Calif. Santa Barbara (Dec. 1997).
9. L. Wolfenstein, *Phys. Rev. D* **17**, 2369 (1978); *Phys. Rev. D* **20**, 2634 (1979); S.P. Mikheyev and A. Yu. Smirnov, *Sov. J. Nucl. Phys.* **42**, 913 (1985); *Nuovo Cimento* **9C**, 17 (1986).
10. N. Hata and P. Langacker, *Phys. Rev. D* **56**, 6107 (1997); N. Hata has done an update for $\nu_e \rightarrow \nu_s$, showing little change.
11. K. Daum *et al.*, *Z. Phys. C* **66**, 417 (1995); M. Aglietta *et al.*, *Europhys. Lett.* **8**, 611 (1989).
12. W.W.M. Allison *et al.*, *Phys. Lett. B* **391**, 491 (1997); H. Gallagher, *WIN '97* (Proc. of Weak Interactions and Neutrino Workshop, Capri, Italy, 1997, in press).
13. R. Becker-Szendy *et al.*, *Phys. Rev. D* **46**, 3720 (1992).
14. Y. Fukuda *et al.*, *Phys. Lett. B* **335**, 237 (1994).
15. E. Kearns, *Proc. of TAUP '97*, LNGS, Assergi, Italy (1997, in press).
16. M. Ambrosio *et al.*, INFN-LNGS preprint INFN/AE-97/21 (to be published in *Proc. of TAUP '97*).
17. M. Appollonio *et al.*, hep-ex/9711002v1, to be published in *Phys. Lett. B*.
18. C. Athanassopoulos *et al.*, *Phys. Rev. C* **54**, 2685 (1996); *Phys. Rev. Lett.* **77**, 3082 (1996).
19. C. Athanassopoulos *et al.*, nucl-ex/9706006 (submitted to *Phys. Rev. C*), nucl-ex/9709006 (submitted to *Phys. Rev. Lett.*).
20. G. Drexlin *et al.*, *Prog. in Part. and Nucl. Phys.* **32**, 375 (1994); B. Armbruster *et al.*, *Nucl. Phys. B* (Proc. Suppl.) **38**, 235 (1995).
21. L. Borodovsky *et al.*, *Phys. Rev. Lett.* **68**, 274 (1992).
22. B. Achkar *et al.*, *Nucl. Phys. B* **434**, 503 (1995).
23. L. DiLella, *Proc of TAUP '97*, LNGS, Assergi, Italy (1997, in press).

24. A. Acker and S. Pakvasa, *Phys. Lett. B* **397**, 209 (1997).
25. C. Cardall and G. Fuller, *Phys. Rev. D* **53**, 4421 (1996).
26. P. Krastev and S. Petcov, *Phys. Lett. B* **397**, 69 (1997); G.L. Fogli, E. Lisi, D. Montanino, and G. Scioscia, *Phys. Rev. D* **56**, 4365 (1997).
27. D.O. Caldwell, *Perspectives in Neutrinos*, Atomic Physics and Gravitation (Editions Frontières, Gif-sur-Yvette, France) p. 187; D.O. Caldwell and R.N. Mohapatra, *Phys. Rev. D* **48**, 3259 (1993); *Phys. Rev. D* **50**, 3477 (1994); J.T. Peltoniemi and J.W.F. Valle, *Nucl. Phys. B* **406**, 409 (1993).
28. A. Klypin, J. Holtzman, J.R. Primack, and E. Regös, *Astrophys. J.* **416**, 1 (1993).
29. A. Klypin, S. Borgani, J. Holtzman, and J.R. Primack, *Astrophys. J.* **444**, 1 (1995).
30. J.R. Primack, J. Holtzman, A. Klypin, and D.O. Caldwell, *Phys. Rev. Lett.* **74**, 2160 (1995).
31. S. Ghigna *et al.*, *Astrophys. J.* **479**, 580 (1997); J.R. Primack, astro-ph/9707285.
32. M.W. Feast and R.W. Catchpole, *Mon. Not. R. Astron. Soc.* **286**, L1 (1997); I.N. Reid, *Astronom. J.* **114**, 161 (1997).
33. S.T. Myers *et al.*, *Astrophys. J.* **485**, 1 (1997).
34. D. Tytler, X.M. Fan, and S. Burles, *Nature* **381**, 207 (1996); *Astrophys. J.* **460**, 584 (1996); D. Tytler, S. Burles, and D. Kirkman, astro-ph/9612121.
35. R. Nolthenius, A.A. Klypin, and J.R. Primack, *Astrophys. J.* **480**, 43 (1997).
36. Y-Z. Qian *et al.*, *Phys. Rev. Lett.* **71**, 1965 (1993); Y.-Z. Qian and G.M. Fuller, *Phys. Rev. D* **51**, 1479 (1995); G. Sigl, *Phys. Rev. D* **51**, 4035 (1995).
37. G.M. Fuller and B.S. Myer, *Astrophys. J.* **453**, 202 (1995); B.S. Myer, G.C. McLaughlin, and G.M. Fuller (in preparation, 1998).
38. D.O. Caldwell, G.M. Fuller, and Y.-Z. Qian (to be submitted to *Phys. Rev. Lett.* 1998).
39. N. Hata, G. Steigman, S. Bludman, and P. Langacker, *Phys. Rev. D* **55**, 540 (1997).
40. R. Foot and R.R. Volkas, *Phys. Rev. D* **56**, 6653 (1997).
41. P. Langacker, Univ. of Penn. preprint UPR0790-T.